



Brief communication: Monitoring snow depth using small, cheap, and easy-to-deploy snow–ground interface temperature sensors

Claire L. Bachand^{1,2}, Chen Wang³, Baptiste Dafflon³, Lauren N. Thomas^{1,4}, Ian Shirley³, Sarah Maebius^{1,5}, Colleen M. Iversen⁶, and Katrina E. Bennett¹

¹Earth and Environmental Sciences, Los Alamos National Laboratory, Los Alamos, NM, USA

²Department of Biology and Wildlife, University of Alaska Fairbanks, Fairbanks, AK, USA

³Earth and Environmental Sciences, Lawrence Berkeley National Laboratory, Berkeley, CA, USA

⁴Department of Geography, University of Colorado Boulder, Boulder, CO, USA

⁵Department of Civil and Environmental Engineering, Princeton University, Princeton, NJ, USA

⁶Environmental Sciences Division and Climate Change Science Institute, Oak Ridge National Laboratory, Oak Ridge, TN, USA

Correspondence: Claire L. Bachand (clbachand@alaska.edu)

Received: 17 July 2024 – Discussion started: 22 August 2024

Revised: 4 November 2024 – Accepted: 12 November 2024 – Published: 28 January 2025

Abstract. Temporally continuous snow depth estimates are vital for understanding changing snow patterns and impacts on permafrost in the Arctic. We trained a random forest machine learning model to predict snow depth from variability in snow–ground interface temperature. The model performed well on Alaska’s Seward Peninsula where it was trained and at Arctic evaluation sites (RMSE ≤ 0.15 m). It performed poorly at temperate sites with deeper snowpacks, partially due to training data limitations. Small temperature sensors are cheap and easy to deploy, so this technique enables spatially distributed and temporally continuous snowpack monitoring at high latitudes to an extent previously infeasible.

1 Introduction

In the Arctic, snow is an important control on permafrost, as it insulates the ground from cold winter temperatures (Shirley et al., 2022a). Changing snow patterns (Bigalke and Walsh, 2022) and associated ground insulation may accelerate permafrost thaw, leading to the release of large amounts of carbon into the atmosphere (Pedron et al., 2023). Further, changing snow seasonality may alter growing season length and carbon uptake by plants (Shirley et al., 2022b). Snow depth is highly variable at fine spatial scales due to drifting that is affected by topography, vegetation, and wind (Ben-

nett et al., 2022). Drifts form in topographic concavities (e.g., stream beds), while tall shrubs entrap blowing snow. As shrubs expand in the Arctic (Mekonnen et al., 2021), the spatial distribution of snow drifts and subsequent impacts on permafrost may change (Lathrop et al., 2024). Thus, monitoring and modeling fine-scale drifting processes are crucial to understanding permafrost evolution.

These processes are poorly characterized in physics-based models (Crumley et al., 2024), and improvements require robust and fine-scale snow depth validation. However, monitoring the spatio-temporal variability of snow remains a challenge. Satellite data can be used to estimate snow depth (Besso et al., 2024), but spatial and temporal resolutions are too coarse to capture the complexity of Arctic snowpacks. End-of-winter snow surveys in remote, high-latitude regions are logistically difficult but capture the fine-scale spatial distribution of peak snow (Bennett et al., 2022). Machine learning (ML) models can be used to extrapolate snow survey data, but these estimates still only represent a single point in time (Bennett et al., 2022). The temporal evolution of snow can be monitored using automated instruments (e.g., snow sonic sensors deployed at Snow Telemetry (SNOTEL) stations; Fleming et al., 2023), but spatially distributed deployment is time-consuming and expensive.

To overcome these challenges, we designed a ML model to extract snow depth from small, inexpensive temperature sen-

sors located at the snow–ground interface. The model was trained at 2 small sites on the Seward Peninsula, Alaska, USA, and evaluated at 10 sites distributed across Alaska, Colorado, and New Mexico (USA); Svalbard (Norway); and Siberia (Russia). Snow dampens temporal variability in snow–ground interface temperature (T_{SG}), and thus snow presence/absence and other snow properties can be identified from T_{SG} data (Lundquist and Lott, 2008; Staub and Delaloye, 2017). Yet, to our knowledge, this is the first time that a complete time series of snow depth has been extracted from T_{SG} measurements alone.

2 Methods

We used data collected at two sites on the Seward Peninsula, Alaska (Fig. S1 in the Supplement): (1) a 2.3 km² gently sloping watershed located at mile marker 27 along the Nome–Teller Highway near Nome, Alaska (hereafter Teller27), and (2) a 2.5 km² hillslope at mile marker 64 of the Nome–Taylor Highway (hereafter Kougark64). According to end-of-winter snow surveys, the average peak snow depth from 2017–2019 at Teller27 was 0.96 m, with an average density of 310 kg m⁻³ (Bennett et al., 2022). In 2018, snow depth was shallower at Kougark64 than at Teller27, with an average end-of-winter depth of 0.75 m and density of 290 kg m⁻³ (Bennett et al., 2022). Vegetation at Teller27 consisted of mixed sedge–willow–*Dryas* tundra and mixed shrub–sedge tussock tundra–bog, with some areas of tall willow shrubs (Bennett et al., 2022). Vegetation at Kougark64 consisted of tussock–lichen tundra, alder savanna, tall willow shrubs in willow–birch tundra, tall alder shrubs in alder shrublands, and rocky areas with birch–ericaceous–lichen and sparse *Dryas*–lichen dwarf shrub tundra (Bennett et al., 2022; Breen et al., 2020).

2.1 Data collection at Teller27 and Kougark64

Collocated snow depth and T_{SG} data were obtained at 151 locations across Teller27 and Kougark64 over the 2021–2022 snow season via distributed temperature profiling (DTP) systems (locations shown in Fig. S1; conceptual schematic in Fig. S2) (Dafflon et al., 2022; Wang et al., 2024b). DTP systems were deployed in late September 2021, and snowfall started on 20 October 2021. DTP systems measured temperatures vertically above the ground in 5 cm increments (seven lowest temperature sensors) to 10 cm increments (eight highest sensors), to a maximum height of 1.67 m. When a sensor is covered by snow, high-frequency fluctuation in temperature drops dramatically, allowing snow depth to be estimated from sensor heights. The estimated snow depths have an uncertainty of ± 2.5 cm or ± 5 cm, depending on the sensor spacing. We estimated T_{SG} from the temperature sensor closest to the snow–ground interface, which ranged from 1 to 5 cm above the ground surface, and thus avoided impacts of

soil or moss on the T_{SG} estimate. Additionally, we extracted shallow subsurface temperature measurements recorded 1 to 5 cm below the ground surface from soil DTP systems deployed into the ground (Wang et al., 2024a). The 15 min DTP data were averaged into 4 h intervals to match the temporal resolution of the miniature temperature sensors described below.

Miniature iButton temperature sensors deployed at the sites (237 total, Figs. S1, S2) recorded T_{SG} from 1 October 2022 to 18 September 2023 in 4 h intervals. iButtons were placed in vacuum-sealed bags and distributed across variable topography and vegetation to capture a broad range of snow conditions. We use the term tall shrubs to refer to deciduous shrubs greater than 0.4 m tall with the capacity to reach heights over 2 m (Sulman et al., 2021). A total of 59 iButtons were placed in tall shrubs (89 outside of tall shrubs) at Teller27, while 41 were placed in tall shrubs (48 outside of tall shrubs) at Kougark64.

2.2 Machine learning model development

Using collocated DTP T_{SG} and snow depth estimates (Sect. 2.1), we developed a random forest ML model to predict snow depth from T_{SG} -derived features, which we refer to hereafter as “RF-Seward”. We also tested a linear model, a simple neural network, and a long short-term memory (LSTM) model. We chose a random forest as it outperformed or performed similarly to other models. A random forest is simple to design, computationally inexpensive, and easy to interpret. We identified key model features using permutation importance, which reflects how model performance changes when an input feature is randomly shuffled (Breiman, 2001). Larger decreases in performances indicate greater feature importance.

We trained RF-Seward on features derived from the 4 h DTP T_{SG} data using the hyperparameter values listed in Table S1 in the Supplement. For each day, we calculated daily T_{SG} maximum and range. We also considered T_{SG} minimum, mean, and standard deviation, but these features were highly correlated (Pearson’s $r > 0.9$) with other higher-performing features. To temporally situate RF-Seward (i.e., incorporate information on neighboring snow conditions) and to smooth its predictions, we included daily T_{SG} standard deviations averaged over a 30 d window (length tuned using the validation dataset) prior to, surrounding, and following each day as features in the model. Further, we tested air-temperature-derived features, but they did not measurably improve RF-Seward. Ultimately, RF-Seward generated a snow depth prediction for each individual day based on the following T_{SG} -derived features (listed in order of permutation feature importance): window surrounding, window following, window prior, daily T_{SG} range, and daily T_{SG} maximum. After finalizing RF-Seward, we retrained the model on all training (96 DTP systems) and validation (24 DTP systems) data and evaluated its performance on the randomly selected test dataset (31 DTP

systems). More details on how the training, validation, and test datasets were applied are available in the Supplement, Fig. S3.

Because temperature sensors are often buried under a small layer of soil to protect them from direct solar radiation or to monitor soil temperatures (e.g., Lundquist and Lott, 2008), we trained a second ML model, which we refer to as “RF-Below”. We used the same hyperparameters and features as RF-Seward but calculated features from shallow subsurface temperatures measured by 95 soil DTP systems (76 training and 19 test systems, locations shown in Fig. S1).

2.3 Additional model evaluation and application to iButtons

2.3.1 Model transferability

To test model transferability, we trained RF-Seward and RF-Below at Teller27 and tested at Kougark64 and vice versa. Further, we applied RF-Seward and RF-Below to 10 evaluation datasets where T_{SG} and snow depth measurements were collocated (within approximately 5 m of each other). Sites were located in the United States (Alaska, Colorado, and New Mexico), Norway (Svalbard) and Russia (Siberia), with temperature sensors placed at the snow–ground interface or within the top 5 cm of soil (see Table S3). Snow depth was also recorded at the sites (e.g., snow sonic sensors at automated weather stations) and was used to evaluate model performance. End-of-season snowpack bulk densities varied among sites and ranged from 180 kg m^{-3} (Samoylov Island, Siberia, Russia) to 450 kg m^{-3} (Senator Beck Basin, CO, USA). Vegetation also varied (Table S3). At Samoylov Island, the temperature sensors were covered by a thick layer of tundra vegetation, while at sites in New Mexico, USA, vegetation consisted of sparse grasses. Prior to this evaluation, we retrained RF-Seward and RF-Below on all available DTP data (training, validation, and test data). By training on all available data, we aimed to maximize model performance by introducing the model to a broader range of snow depths and temperature responses.

2.3.2 Performance in deep snow

The training data at our study sites were limited to a maximum of 1.77 m due to the length of DTP system probes, and thus RF-Seward and RF-Below cannot predict depths greater than 1.77 m. To test if ML could accurately predict deeper snow depths, we trained a third ML model, which we refer to as “RF-Deep”. To train this model, we supplemented our original Seward Peninsula training dataset with additional data from two model evaluation sites in Senator Beck Basin, CO, USA, with deeper snowpacks (Table S3). The model was applied to one site and trained with data from the other (in addition to the Seward Peninsula DTP data). To mimic the distribution of snow depths at these sites, we en-

sured that 10 % of the training data consisted of snow depths above 2 m. This reduced the training dataset size compared to other models (Table S2).

2.3.3 Model application to iButtons

We applied RF-Seward to iButtons deployed at Teller27 and Kougark64 (Sect. 2.1) to assess how tall shrubs affect snow depth and T_{SG} . We divided the iButtons into two groups: within and outside of tall shrubs. We averaged T_{SG} measurements and snow depth predictions over a period corresponding to peak snow (20 March–9 April). We used the non-parametric Wilcoxon rank-sum test (Wilcoxon, 1945) to identify statistical differences in snow and T_{SG} conditions between shrubs and no shrubs.

3 Results and discussion

RF-Seward performed well on the test dataset ($R^2 = 0.87$; RMSE = 0.15 m; mean bias = 0.03 m; Fig. 1a) but underestimated snow depths when trained at Teller27 and tested at Kougark64 ($R^2 = 0.85$; RMSE = 0.17 m; mean bias = -0.10 m; Fig. 1b) and overestimated snow depths when trained at Kougark64 and tested at Teller27 ($R^2 = 0.72$; RMSE = 0.22 m; mean bias = 0.05 m; Fig. 1c). Differing air temperature regimes between Teller27 (warmer) and Kougark64 (colder) may have contributed to these biases (i.e., the same snow depth at the two locations corresponded to different T_{SG}). However, all RF-Seward features were derived from T_{SG} variability (not magnitudes), except for T_{SG} maximum. Excluding T_{SG} maximum from the model (not shown) did not eliminate the biases seen in Fig. 1b, c, suggesting that these errors may be tied to factors that affect T_{SG} ranges (e.g., latent heat processes). RF-Below performed worse than RF-Seward and did not transfer as well between sites (Fig. 1d–f), likely due to variability in ground insulation properties (i.e., soil type, vegetation, etc.), which confound the snow insulation effect. Further, warmer and/or wetter sites (e.g., Teller27) undergo more freezing and thawing than colder and/or drier sites (e.g., Kougark64), producing zero-curtain periods where the key snow depth predictor (temperature variability) flattens at 0°C as water changes phase (Staub and Delaloye, 2017).

RF-Seward performed well at the two sites where T_{SG} data were available in the Arctic: Bayelva Station in Norway (RMSE = 0.15 m; mean bias = 0.02 m; Fig. 2a) and Imnavait Creek, on Alaska’s North Slope (RMSE = 0.08 m; mean bias = -0.04 m; Fig. 2b), indicating that the model may be transferable to other pan-Arctic locations. Additionally, we tested RF-Seward and RF-Below at four sites in the Arctic where temperature was recorded below the ground surface. At Samoylov Island, Russia (Fig. 2e), sensors were placed below an insulating layer of wet tundra vegetation, which caused RF-Seward to overpredict snow depth

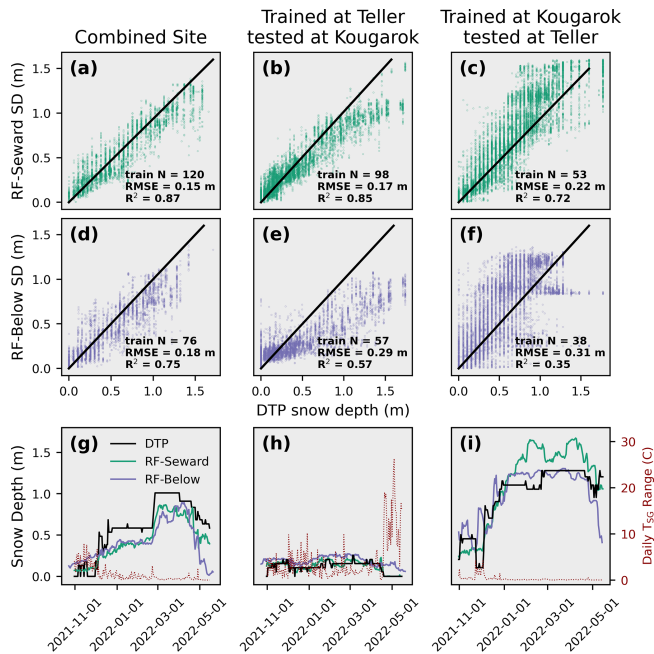


Figure 1. Performance of RF-Seward (a) evaluated using test data, (b) when trained at Teller27 and tested at Kougarok64 and (c) vice versa. (d–f) Same as (a)–(c) but for RF-Below. Time series plots of DTP snow depth data vs. ML estimates when (g) trained at both sites, (h) at Teller2, and (i) at Kougarok64. The dotted red line shows the daily T_{SG} range, with narrower temperature ranges occurring under deeper snow cover. “Train N” refers to the number of DTP sensors used to train each model.

(mean bias = 0.40 m). RF-Below decreased overestimations at Samoylov Island (mean bias = 0.14 m) and at other sites in Alaska (Fig. 2c, d, f). RF-Below performed best at sites near Council on the Seward Peninsula, Alaska, USA, likely because vegetation at these sites is most similar to vegetation at the training study sites.

In New Mexico, USA, paired iButtons recorded above- and belowground temperature data at two sites (A and B). Predictions from iButtons placed above the ground surface were averaged into a single RF-Seward estimate, while predictions from iButtons placed below the ground surface were averaged into a single RF-Below estimate. At Site B, RF-Seward and RF-Below underpredicted peak snow by about 0.07 m (Fig. 2g). RF-Seward performed better at Site A (observed peak snow = 0.18 m; predicted = 0.16 m), although RF-Below still underpredicted peak snow by 0.10 m, possibly because the model expected insulating tundra vegetation. Both models performed worse when applied in the wrong context (i.e., RF-Seward overpredicted peak snow by 0.13 m when applied to belowground data; RF-Below underpredicted peak snow by 0.16 m when applied to aboveground data), indicating that excess insulation from a thin layer of soil or vegetation will be confused for snow.

Performance at the New Mexico, USA, sites fell within RF-Seward and RF-Below’s typical ranges, despite the higher end-of-season bulk density compared to Arctic snow ($\sim 400 \text{ kg m}^{-3}$ vs. 300 kg m^{-3}). However, zero-curtain periods (ZCPs) caused the model to occasionally overestimate snow depth. For the aboveground iButtons, ZCPs were likely caused by water pooling and freezing on top of the iButton’s vacuum-sealed bag and by water freezing at the bottom of the snowpack following rain on snow (ROS; Staub and Delaloye, 2017). In New Mexico, USA, ROS occurred from 21–25 January 2024, leading to an erroneous snow accumulation event in Fig. 2g. ZCPs were more prevalent in the belowground data due to the repetitive freeze–thaw of the soils during snow-free periods of the winter, causing erroneous RF-Below predictions (e.g., early snow accumulation in Fig. 2g). Our results suggest that RF-Below will perform poorly for warm, ephemeral snowpacks, which are expected to become more common as the climate warms (Wieder et al., 2022). ZCPs completely dampen T_{SG} variability and therefore uncouple T_{SG} from snow depth. Even given training data more representative of ZCPs, snow depth estimates may remain unreliable during these periods. Incorporating features into the model which indicate the presence of ZCPs may reduce these errors. Further, deploying iButtons at the snow–ground interface (rather than below the ground) decreases the number of ZCPs in the temperature data.

Belowground temperature data were recorded at Grand Mesa, Colorado, USA (Fig. 2h), while T_{SG} was recorded at two sites in Senator Beck Basin, Colorado, USA (Fig. 2i–j). These sites accumulated more snow (up to 2.85 m) than the sites where RF-Seward was trained (maximum depth = 1.77 m), resulting in underpredictions of deep snow at these sites (Fig. 2h–j). RF-Deep predicted deeper snow depths than RF-Seward, although predictions still leveled off prematurely for some years (e.g., 2008–2009 in Fig. 2j). RF-Deep also appeared visually noisy compared to RF-Seward, possibly due to the smaller training dataset (Table S2) and lower-quality training data (i.e., temperature and snow depth measurements were not perfectly collocated). RF-Deep’s poor performance indicates that at a certain depth, T_{SG} may be dampened to the extent that ML can no longer accurately predict snow depth. Past research has shown that snow depths greater than 0.5 m can completely insulate the ground, although even snowpacks deeper than 4 m are not always fully insulating (Slater et al., 2017; Staub and Delaloye, 2017, their Fig. 5). Because of this, it is likely that deep snow decreases the predictive value of T_{SG} measurements, which will have a minimal effect on understanding soil temperature but could cause major errors when estimating water availability from snow depth predictions.

Model application to iButtons

Shrubs can entrain blowing snow, resulting in snow drifts (Bennett et al., 2022). Averaged from 20 March–

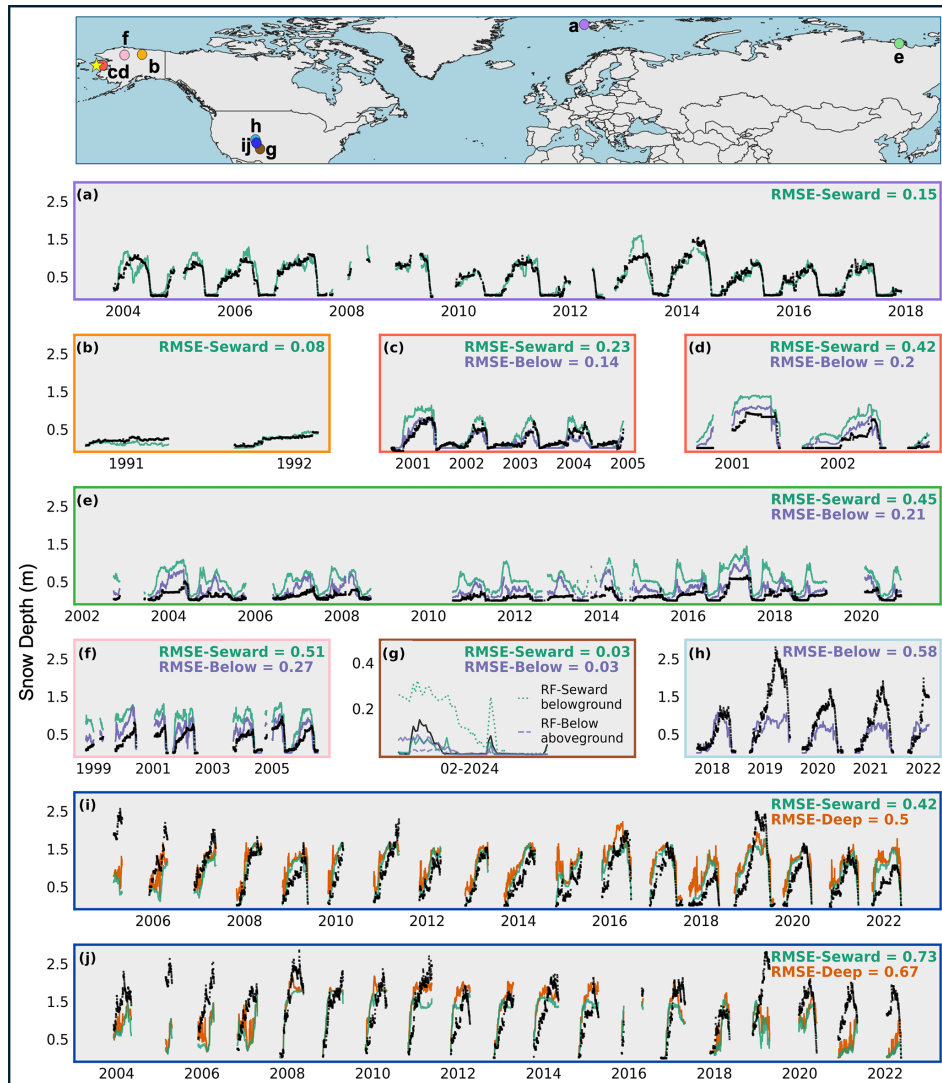


Figure 2. ML performance at (a) Bayelva Station, Svalbard, Norway (Boike et al., 2017, 2018); (b) Innavaik Creek, Alaska, USA (Sturm and Holmgren, 1994; Stuefer et al., 2020); (c, d) Council, Alaska, USA (Hinzman et al., 2016); (e) Samoylov Island, Siberia, Russia (Boike et al., 2019a, b); (f) Ivotuk, Alaska, USA (Hinzman et al., 2016); (g) Los Alamos, New Mexico, USA (Thomas et al., 2024); (h) Grand Mesa, Colorado, USA (Houser et al., 2022); and (i, j) Senator Beck Basin, Colorado, USA (Center for Snow and Avalanche Studies, 2024; Landry et al., 2014). Locations are shown on a map, with the yellow star indicating the Seward Peninsula of Alaska, USA, where RF-Seward was trained. The black lines show measured snow depth at each site. The y-axis and RMSE values indicate snow depth in meters. Note the adjusted y axis for Los Alamos, New Mexico, USA (g). For this site, we also show RF-Seward and RF-Below predictions when RF-Below was applied above the ground and RF-Seward was applied below the ground (dotted lines).

9 April 2023, the ML model estimated 0.29 m more snow for iButtons deployed in tall shrubs than outside of tall shrubs ($p < 0.001$). This result may be biased low as RF-Seward rarely predicted more than 1.5 m of snow due to training data limitations. T_{SG} averaged from 20 March to 9 April was 1.94 °C warmer in tall shrubs than outside of tall shrubs ($p < 0.001$). This provides evidence that increasing Arctic shrubification (Mekonnen et al., 2021) may increase snow depths, insulate the subsurface in winter, and accelerate permafrost thaw as suggested by Sturm et al. (2001). However,

topographic and landscape characteristics can drive the formation of deep snow drifts even without the presence of tall shrubs (Parr et al., 2020). The iButton with the fourth-highest snow depth prediction, averaged from 20 March to 9 April (1.45 m), was placed in short grasses adjacent to a stream bed, which likely experienced snow drifting due to topographic concavity (Parr et al., 2020). Similarly, the iButton with the fifth-highest snow depth prediction (1.44 m) was placed near the edge of dense tall shrubs, where snow may have also accumulated (Currier and Lundquist, 2018).

4 Conclusions

We trained a ML model to predict snow depth from variability in snow–ground interface temperature. The model performed well on the test dataset and at two Arctic evaluation sites ($RMSE \leq 0.15$ m). Small temperature sensors are cheap and easy to deploy, so this technique enabled spatially distributed and temporally continuous snowpack monitoring to an extent previously infeasible. Additional collocated T_{SG} and snow depth observations could be used to retrain the model and enhance its transferability. While the model generally performed well, rain on snow and zero-curtain periods caused the model to erroneously predict snow accumulation events. Further, the model failed to replicate deep snow (greater than 1.5 m) observed in Colorado, USA. For optimal performance, the model should be applied to temperatures recorded at the snow–ground interface. Predictions made using subsurface temperatures were impacted by varying soil types, vegetation properties, and latent heat processes. Using ML predictions, we found that snow at Teller27 and Kougarak64 was significantly deeper in patches of tall shrubs than outside of tall shrubs, and T_{SG} averaged from 20 March to 9 April was on average 1.94 °C warmer within tall shrubs.

Future research should focus on developing this technique for locations where peak snow depths exceed 1.5 m (e.g., Colorado, USA), as these regions are crucial for water security across the world. While deep snow may completely dampen T_{SG} , it is possible that the ML model will perform better given a larger and more representative training dataset and/or additional input features. Alternatively, this technique could be combined with other monitoring and/or modeling efforts. For example, snow depth estimates made early in the snow season (e.g., when snow is shallow) could be used to estimate snow variability across the landscape and to downscale coarse model or remote sensing snow depth estimates. Further, the application of a ML model tailored towards time series estimates (e.g., a long short-term memory model; LSTM) could improve predictions. In this study, we only had 1 year of data, which likely limited the LSTM's performance. With a longer-term dataset, we could provide the LSTM with more training points and a longer look-back window (e.g., an entire snow season), which would likely enhance its performance. Additionally, how snow stratigraphy and density affect model results remains unclear. The sites examined here typically experienced frozen soil prior to snowmelt, and therefore, how unfrozen soils affect ML predictions should also be explored.

Code and data availability. Snow depth predictions are available on the Environmental System Science Data Infrastructure for a Virtual Ecosystem (ESS-DIVE) data portal (Bachand et al., 2024; <https://doi.org/10.15485/2371854>). The data package includes a *.csv file of RF-Seward and RF-Below predictions at sites in the United States (Alaska, Colorado, and New Mexico), Norway, and Russia (Siberia). The machine learning model is available on GitHub (<https://github.com/cbachand-LANL/iButton-SnowDepth-ML>, last access: 22 January 2025, <https://doi.org/10.5281/zenodo.14657741>, Bachand, 2025). The code package includes a *.joblib file of the trained RF-Seward model, which can be downloaded and directly applied to new datasets. Example workflows for cleaning data inputs, training machine learning models, and making predictions are also included in an *.ipynb file. iButton temperature measurements at Teller27 and Kougarak64 (Bennett et al., 2024; <https://doi.org/10.15485/2319246>) and at the Los Alamos, New Mexico, USA, study sites (Thomas et al., 2024; <https://doi.org/10.15485/2338028>) are available on ESS-DIVE, together with the DTP temperature and snow depth data used in this study (<https://doi.org/10.15485/2475020>, Wang et al., 2024b).

Supplement. The supplement related to this article is available online at: <https://doi.org/10.5194/tc-19-393-2025-supplement>.

Author contributions. CLB wrote the manuscript draft, developed the random forest methodology, and performed analysis; CW developed the methodology to estimate snow depth using DTP and curated data; BD, CW, and IS led the DTP system deployment, data collection, and data analysis; LNT led the iButton data collection campaigns in Los Alamos, NM, USA; SM developed the LSTM methodology; CMI acquired funding and is the PI of the NGEE Arctic project; KEB developed the data collection study at Teller27 and Kougarak64, supervised research, developed the research concept, contributed original text, and is the institutional lead of the NGEE Arctic project at LANL; all authors reviewed and edited the paper.

Competing interests. The contact author has declared that none of the authors has any competing interests.

Disclaimer. Publisher's note: Copernicus Publications remains neutral with regard to jurisdictional claims made in the text, published maps, institutional affiliations, or any other geographical representation in this paper. While Copernicus Publications makes every effort to include appropriate place names, the final responsibility lies with the authors.

Acknowledgements. We gratefully acknowledge Mary's Igloo (Qawiaraq in Inupiaq), Sitnasuak, and Council Native Corporations for guidance and for allowing us to conduct our research on their traditional lands. The authors gratefully acknowledge the contributions of Shannon Dillard, Ryan Crumley, Eve Gasarch, Evan Thaler, Jerome Quintana, Kenneth Waight, Stijn Wielandt, John Lamb, Syl-

vain Fiolleau, Sebastian Uhlemann, and Craig Ulrich for assisting in data collection at the Teller27, Kougarok64, and Los Alamos (New Mexico, USA) study sites. We thank Mia Mitchell for her assistance with Fig. S1. Further, we thank Julia Boike and Mathew Sturm for providing insight and data sources as we developed this machine learning approach.

Financial support. The Next-Generation Ecosystem Experiments in the Arctic (NGEE Arctic) project is supported by the Office of Biological and Environmental Research in the US Department of Energy’s Office of Science.

Review statement. This paper was edited by Chris Derksen and reviewed by three anonymous referees.

References

- Bachand, C.: cbachand-LANL/iButton-SnowDepth-ML: Code for “Brief Communication: Monitoring snow depth using small, cheap, and easy-to-deploy snow-ground interface temperature sensors” (v1.0.0), Zenodo [code], <https://doi.org/10.5281/zenodo.14657741>, 2025.
- Bachand, C., Wang, C., Dafflon, B., Thomas, L., Shirley, I., Maebius, S., Iversen, C., and Bennett, K.: Machine learning snow depth predictions at sites in Alaska, Norway, Siberia, Colorado and New Mexico, Next-Generation Ecosystem Experiments (NGEE) Arctic, ESS-DIVE repository [data set], <https://doi.org/10.15485/2371854>, 2024.
- Bennett, K. E., Miller, G., Busey, R., Chen, M., Lathrop, E. R., Dann, J. B., Nutt, M., Crumley, R., Dillard, S. L., Dafflon, B., Kumar, J., Bolton, W. R., Wilson, C. J., Iversen, C. M., and Wullschleger, S. D.: Spatial patterns of snow distribution in the sub-Arctic, *The Cryosphere*, 16, 3269–3293, <https://doi.org/10.5194/tc-16-3269-2022>, 2022.
- Bennett, K., Bachand, C., Thomas, L., Gasarch, E., Thaler, E., and Crumley, R.: iButton and Tinytag snow/ground interface temperature measurements at Teller 27 and Kougarok 64 from 2022–2023, Next-Generation Ecosystem Experiments (NGEE) Arctic, ESS-DIVE repository [data set], <https://doi.org/10.15485/2319246>, 2024.
- Besso, H., Shean, D., and Lundquist, J. D.: Mountain snow depth retrievals from customized processing of ICESat-2 satellite laser altimetry, *Remote Sens. Environ.*, 300, 113843, <https://doi.org/10.1016/j.rse.2023.113843>, 2024.
- Bigalke, S. and Walsh, J. E.: Future Changes of Snow in Alaska and the Arctic under Stabilized Global Warming Scenarios, *Atmosphere*, 13, 541, <https://doi.org/10.3390/atmos13040541>, 2022.
- Boike, J., Juszak, I., Lange, S., Chadburn, S., Burke, E. J., Overduin, P. P., Roth, K., Ippisch, O., Bornemann, N., Stern, L., Gouttevin, I., Hauber, E., and Westermann, S.: Measurements in soil and air at Bayelva Station, PANGAEA [data set], <https://doi.org/10.1594/PANGAEA.880120>, 2017.
- Boike, J., Juszak, I., Lange, S., Chadburn, S., Burke, E., Overduin, P. P., Roth, K., Ippisch, O., Bornemann, N., Stern, L., Gouttevin, I., Hauber, E., and Westermann, S.: A 20-year record (1998–2017) of permafrost, active layer and meteorological conditions at a high Arctic permafrost research site (Bayelva, Spitsbergen), *Earth Syst. Sci. Data*, 10, 355–390, <https://doi.org/10.5194/essd-10-355-2018>, 2018.
- Boike, J., Nitzbon, J., Anders, K., Grigoriev, M., Bolshiyarov, D., Langer, M., Lange, S., Bornemann, N., Morgenstern, A., Schreiber, P., Wille, C., Chadburn, S., Gouttevin, I., Burke, E., and Kutzbach, L.: A 16-year record (2002–2017) of permafrost, active-layer, and meteorological conditions at the Samoylov Island Arctic permafrost research site, Lena River delta, northern Siberia: an opportunity to validate remote-sensing data and land surface, snow, and permafrost models, *Earth Syst. Sci. Data*, 11, 261–299, <https://doi.org/10.5194/essd-11-261-2019>, 2019a.
- Boike, J., Nitzbon, J., Bolshiyarov, D., Langer, M., Lange, S., Bornemann, N., Morgenstern, A., Schreiber, P., Wille, C., Chadburn, S., Gouttevin, I., and Kutzbach, L.: Measurements in soil and air at Samoylov Station (2002–2018), version 201908, Alfred Wegener Institute – Research Unit Potsdam, PANGAEA [data set], <https://doi.org/10.1594/PANGAEA.905236>, 2019b.
- Breiman, L.: Random Forests, *Mach. Learn.*, 45, 5–32, <https://doi.org/10.1023/A:1010933404324>, 2001.
- Breen, A., Iversen, C., Salmon, V., Stel, H. V., Busey, B., and Wullschleger, S.: NGEE Arctic Plant Traits: Plant Community Composition, Kougarok Road Mile Marker 64, Seward Peninsula, Alaska, 2016, Next-Generation Ecosystem Experiments (NGEE) Arctic, ESS-DIVE repository [data set], <https://doi.org/10.5440/1465967>, 2020.
- Center for Snow and Avalanche Studies: Archival Data from Senator Beck Basin Study Area, <https://snowstudies.org/archival-data/> (last access: 1 July 2024), 2024.
- Crumley, R., Bachand, C., and Bennett, K. E.: Snow distribution patterns revisited: A physics-based and machine learning hybrid approach to snow distribution mapping in the sub-Arctic, *Water Resour. Res.*, 60, e2023WR036180, <https://doi.org/10.1029/2023WR036180>, 2024.
- Currier, W. R. and Lundquist, J. D.: Snow Depth Variability at the Forest Edge in Multiple Climates in the Western United States, *Water Resour. Res.*, 54, 8756–8773, <https://doi.org/10.1029/2018WR022553>, 2018.
- Dafflon, B., Wielandt, S., Lamb, J., McClure, P., Shirley, I., Uhlemann, S., Wang, C., Fiolleau, S., Brunetti, C., Akins, F. H., Fitzpatrick, J., Pullman, S., Busey, R., Ulrich, C., Peterson, J., and Hubbard, S. S.: A distributed temperature profiling system for vertically and laterally dense acquisition of soil and snow temperature, *The Cryosphere*, 16, 719–736, <https://doi.org/10.5194/tc-16-719-2022>, 2022.
- Fleming, S. W., Zukiewicz, L., Strobel, M. L., Hofman, H., and Goodbody, A. G.: SNOTEL, the Soil Climate Analysis Network, and water supply forecasting at the Natural Resources Conservation Service: Past, present, and future, *J. Am. Water Resour. As.*, 59, 585–599, <https://doi.org/10.1111/1752-1688.13104>, 2023.
- Hinzman, L. D., Kane, D. L., and Goering, D. J.: Meteorological, Radiation, Soil, and Snow Data from Alaska Sites, 1998–2008, Arctic Data Center [data set], <https://doi.org/10.5065/D6G44NFV>, 2016.
- Houser, P., Rudisill, W., Johnston, J., Elder, K., Marshall, H. P., Vuyovich, C., Kim, E., and Mason, M.: SnowEx Meteorological Station Measurements from Grand Mesa, CO, Version 1, NASA National Snow and Ice Data Center Distributed Active Archive

- Center [data set], <https://doi.org/10.5067/497NQVJ0CBEX>, 2022.
- Landry, C. C., Buck, K. A., Raleigh, M. S., and Clark, M. P.: Mountain system monitoring at Senator Beck Basin, San Juan Mountains, Colorado: A new integrative data source to develop and evaluate models of snow and hydrologic processes, *Water Resour. Res.*, 50, 1773–1788, <https://doi.org/10.1002/2013WR013711>, 2014.
- Lathrop, E., Thomas, L., Gasarch, E., Bachand, C., Bolton, W. R., Busey, R., Crumley, R. L., Dann, J., Dillard, S. L., and Bennett, K. E.: Shrubs Strongly Influence Snow Properties in Two Subarctic Watersheds, *Permafrost Periglac.*, 1–16, <https://doi.org/10.1002/ppp.2263>, online first, 2024.
- Lundquist, J. D. and Lott, F.: Using inexpensive temperature sensors to monitor the duration and heterogeneity of snow-covered areas, *Water Resour. Res.*, 44, W00D16, <https://doi.org/10.1029/2008WR007035>, 2008.
- Mekonnen, Z. A., Riley, W. J., Berner, L. T., Bouskill, N. J., Torn, M. S., Iwahana, G., Breen, A. L., Myers-Smith, I. H., Criado, M. G., and Liu, Y.: Arctic tundra shrubification: a review of mechanisms and impacts on ecosystem carbon balance, *Environ. Res. Lett.*, 16, 053001, <https://doi.org/10.1088/1748-9326/abf28b>, 2021.
- Parr, C., Sturm, M., and Larsen, C.: Snowdrift Landscape Patterns: An Arctic Investigation, *Water Resour. Res.*, 56, e2020WR027823, <https://doi.org/10.1029/2020WR027823>, 2020.
- Pedron, S. A., Jespersen, R. G., Xu, X., Khazindar, Y., Welker, J. M., and Czimczik, C. I.: More Snow Accelerates Legacy Carbon Emissions From Arctic Permafrost, *AGU Adv.*, 4, e2023AV000942, <https://doi.org/10.1029/2023AV000942>, 2023.
- Shirley, I. A., Mekonnen, Z. A., Wainwright, H., Romanovsky, V. E., Grant, R. F., Hubbard, S. S., Riley, W. J., and Dafflon, B.: Near-Surface Hydrology and Soil Properties Drive Heterogeneity in Permafrost Distribution, Vegetation Dynamics, and Carbon Cycling in a Sub-Arctic Watershed, *J. Geophys. Res.-Biogeo.*, 127, e2022JG006864, <https://doi.org/10.1029/2022JG006864>, 2022a.
- Shirley, I. A., Mekonnen, Z. A., Grant, R. F., Dafflon, B., Hubbard, S. S., and Riley, W. J.: Rapidly changing high-latitude seasonality: implications for the 21st century carbon cycle in Alaska, *Environ. Res. Lett.*, 17, 014032, <https://doi.org/10.1088/1748-9326/ac4362>, 2022b.
- Slater, A. G., Lawrence, D. M., and Koven, C. D.: Process-level model evaluation: a snow and heat transfer metric, *The Cryosphere*, 11, 989–996, <https://doi.org/10.5194/tc-11-989-2017>, 2017.
- Staub, B. and Delaloye, R.: Using Near-Surface Ground Temperature Data to Derive Snow Insulation and Melt Indices for Mountain Permafrost Applications: Snow and Melt Indices Derived from GST Data, *Permafrost Periglac.*, 28, 237–248, <https://doi.org/10.1002/ppp.1890>, 2017.
- Stuefer, S. L., Kane, D. L., and Dean, K. M.: Snow Water Equivalent Measurements in Remote Arctic Alaska Watersheds, *Water Resour. Res.*, 56, e2019WR025621, <https://doi.org/10.1029/2019WR025621>, 2020.
- Sturm, M. and Holmgren, J.: Effects of microtopography on texture, temperature and heat flow in Arctic and sub-Arctic snow, *Ann. Glaciol.*, 19, 63–68, <https://doi.org/10.3189/1994AoG19-1-63-68>, 1994.
- Sturm, M., Holmgren, J., McFadden, J. P., Liston, G. E., Chapin, F. S., and Racine, C. H.: Snow–Shrub Interactions in Arctic Tundra: A Hypothesis with Climatic Implications, *J. Climate*, 14, 336–344, [https://doi.org/10.1175/1520-0442\(2001\)014<0336:SSIIAT>2.0.CO;2](https://doi.org/10.1175/1520-0442(2001)014<0336:SSIIAT>2.0.CO;2), 2001.
- Sulman, B. N., Salmon, V. G., Iversen, C. M., Breen, A. L., Yuan, F., and Thornton, P. E.: Integrating Arctic Plant Functional Types in a Land Surface Model Using Above- and Belowground Field Observations, *J. Adv. Model. Earth Sy.*, 13, e2020MS002396, <https://doi.org/10.1029/2020MS002396>, 2021.
- Thomas, L., Bachand, C., and Maebius, S.: iButton snow-ground interface temperature measurements in Los Alamos, New Mexico from 2023 - 2024., Next-Generation Ecosystem Experiments (NGEE) Arctic, ESS-DIVE repository [data set], <https://doi.org/10.15485/2338028>, 2024.
- Wang, C., Shirley, I., Wielandt, S., Lamb, J., Uhlemann, S., Breen, A., Busey, R. C., Bolton, W. R., Hubbard, S., and Dafflon, B.: Local-scale heterogeneity of soil thermal dynamics and controlling factors in a discontinuous permafrost region, *Environ. Res. Lett.*, 19, 034030, <https://doi.org/10.1088/1748-9326/ad27bb>, 2024a.
- Wang, C., Dafflon, B., Shirley, I., Wielandt, S., Fiolleau, S., Lamb, J., Uhlemann, S., and Ulrich, C.: Continuous snow depth, ground interface temperature and shallow soil temperature measurements from 2021-10-1 to 2022-6-14, Seward Peninsula, Alaska, Next-Generation Ecosystem Experiments (NGEE) Arctic, ESS-DIVE repository [data set], <https://doi.org/10.15485/2475020>, 2024b.
- Wieder, W. R., Kennedy, D., Lehner, F., Musselman, K. N., Rodgers, K. B., Rosenbloom, N., Simpson, I. R., and Yamaguchi, R.: Pervasive alterations to snow-dominated ecosystem functions under climate change, *P. Natl. Acad. Sci. USA*, 119, e2202393119, <https://doi.org/10.1073/pnas.2202393119>, 2022.
- Wilcoxon, F.: Individual Comparisons by Ranking Methods, *Biom. Bull.*, 1, 80–83, <https://doi.org/10.2307/3001968>, 1945.